

## Comparison of High Pressure-Induced Phases of $\text{Mg}(\text{AlH}_4)_2$ as Hydrogen Storage Using Ab Initio Calculated NQCC Parameters

Marjan A. Rafiee

Department of Chemistry, Payame Noor University, P.O. BOX 19395-3697 Tehran, Iran

e-mail: rafiee.marjan@gmail.com

Published online: 15 November 2017

To cite this article: Rafiee, M. A. (2017). Comparison of high pressure-induced phases of  $\text{Mg}(\text{AlH}_4)_2$  as hydrogen storage using ab initio calculated NQCC parameters. *J. Phys. Sci.*, 28(3), 69–79, <https://doi.org/10.21315/jps2017.28.3.5>

To link to this article: <https://doi.org/10.21315/jps2017.28.3.5>

**ABSTRACT:** Nuclear quadrupole resonance (NQR) spectroscopy is proven to be a very sensitive technique for measuring distribution of electric charge around quadrupolar nuclei. Quadrupolar parameters of nuclei can be used as a tool to understand the electronic structure of compounds. The electronic structure of magnesium alanate,  $\text{Mg}(\text{AlH}_4)_2$ , as promising hydrogen storage materials for hydrogen fuel cell-powered automobile applications, has been studied in detail by ab initio calculated NQR parameters. Furthermore, using calculated nuclear quadrupole coupling constants (NQCCs) of hydrogen atoms ( $^2\text{H}$ -NQCC), the electronic structure of  $\alpha$ - $\text{Mg}(\text{AlH}_4)_2$  with its high-pressure forms,  $\beta$ - and  $\gamma$ - $\text{Mg}(\text{AlH}_4)_2$ , was compared. The electric field gradient (EFG) at the site of  $^2\text{H}$  atoms was calculated to obtain NQCC parameters. The results show that in the  $\gamma$ - $\text{Mg}(\text{AlH}_4)_2$ ,  $^2\text{H}$ -NQCCs are smaller than that of other considered phases. In other words, Al–H bonds in  $\gamma$ - $\text{Mg}(\text{AlH}_4)_2$  nanocrystal is weaker than others and the charge transfer from Al to hydrogen atom is less than the others and therefore these hydrogens have weaker bonds with Al and easier condition for dehydrogenation is expected in  $\gamma$ - $\text{Mg}(\text{AlH}_4)_2$ . Comparison of calculated dehydrogenation enthalpies of various  $\text{Mg}(\text{AlH}_4)_2$  phases verifies this prediction. All calculations performed using Gaussian 03 at the HF/3-21G level of theory. The selected level and basis set give the rather acceptable qualitative NQCCs of hydrogen atoms.

**Keywords:** Nuclear quadrupole resonance,  $\text{Mg}(\text{AlH}_4)_2$ , hydrogen, ab initio calculations,  $^2\text{H}$ -NQCC

## 1. INTRODUCTION

The alanates (complex aluminohydrides) possess a relatively high gravimetric hydrogen density. They are also considered among the most promising solid-state hydrogen-storage materials. Studies show that alanates such as  $\text{LiAlH}_4$  and  $\text{Mg}(\text{AlH}_4)_2$  are promising hydrogen storage materials in hydrogen fuel cell-powered automobile applications.<sup>1-12</sup>  $\text{Mg}(\text{AlH}_4)_2$  possesses a very high theoretical hydrogen capacity (9.3%) and low decomposition temperature ( $<150^\circ\text{C}$ ).<sup>8-11</sup>  $\text{Mg}(\text{AlH}_4)_2$  was first synthesised in 1950 by Wiberg and Bauer, while its thermal decomposition behaviour was also studied.<sup>6,9,10,13</sup> The crystal structure of  $\text{Mg}(\text{AlH}_4)_2$  (hereafter,  $\alpha\text{-Mg}(\text{AlH}_4)_2$ ) has been determined by X-ray and neutron diffraction experiments.<sup>14</sup> Using ab initio methods, the electronic structure and vibrational properties of some magnesium alanates were studied by Setten et al., and Spano and Bernasconi, respectively.<sup>15,16</sup> It is known that  $\text{Mg}(\text{AlH}_4)_2$  retains a higher capacity for hydrogen storage compared to sodium alanate.<sup>17,18</sup> It was also reported that  $\text{Mg}(\text{AlH}_4)_2$  readily decomposes at temperatures below  $200^\circ\text{C}$ .<sup>10</sup>

Experiments on X-ray powder-diffraction found that, under ambient conditions, the  $\alpha\text{-Mg}(\text{AlH}_4)_2$  structure (Figure 1) exhibits the space-group symmetry  $P\bar{3}m1$  with a  $\text{CdI}_2$ -layered structure. Except for  $\text{Ca}(\text{BF}_4)_2$ -type structure, in which magnesium atom located at the centre of a distorted square anti-prism is coordinated by eight H atoms, in  $\alpha\text{-Mg}(\text{AlH}_4)_2$  and other proposed magnesium alanates, there almost exist two kinds of polyhedral. First is the  $\text{AlH}_4$  tetrahedron in which the aluminium atom is tetrahedrally coordinated by one H1 and three H2 atoms. Second is the  $\text{MgH}_6$  octahedron in which the magnesium atom is octahedrally coordinated by six  $\text{H}_2$  atoms.<sup>19</sup>

Calculations on the total energy indicate that under ambient pressure the structure of  $\alpha\text{-Mg}(\text{AlH}_4)_2$  found by experiments is more stable than the other proposed structures.<sup>19</sup> Nevertheless, despite these detailed studies and the promise of magnesium aluminium hydride systems, there remain still considerable challenges, which are impeded by uncertainties about thermodynamic and kinetic parameters of removing hydrogen from them and adding hydrogen to them. Hu et al. showed that with pressure increasing the structural transition from  $\alpha$ - to  $\beta$ -  $\text{Mg}(\text{AlH}_4)_2$  ( $\delta\text{-Zr}(\text{MoO}_4)_2$ -type structure) and then  $\beta$ - to  $\gamma$ -  $\text{Mg}(\text{AlH}_4)_2$  ( $\text{Ca}(\text{BF}_4)_2$ -type structure) occur at 0.67 and 10.28 GPa respectively, accompanied by volume reductions of 6.6% and 8.7%.<sup>19</sup>

Understanding the bonding nature of aluminium and hydrogen is essential in order to improve its fundamental dehydrogenation performance. To further understand the nature of the bonding, charge density distribution is typically investigated by Nuclear Quadrupole Resonance (NQR) spectroscopy analysis.<sup>20</sup>

NQR spectroscopy is a very sensitive technique for measurement of the electric charge distribution around quadrupolar nuclei ( $I > 1/2$ ).<sup>21</sup>

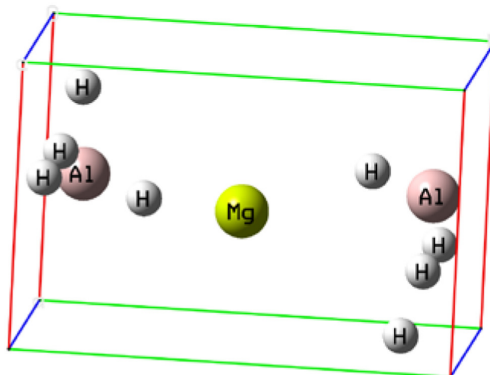


Figure 1: Crystal structure of  $\alpha$ -Mg(AlH<sub>4</sub>)<sub>2</sub> modification.

The quantum mechanical approach is an effective method in determination of the charge distribution in molecules or complexes.<sup>22</sup> In this method, the electric field gradient (EFG), resulting from whole molecular charges, can be estimated at any point in the molecular space.<sup>23</sup> Verification of the EFG has become possible by the quadrupolar nuclei which possess a nuclear quadrupole moment and interact with molecular EFG tensor.<sup>23</sup> This interaction is measured by the nuclear quadrupole coupling constant (NQCC).

NQCC tensor is the energy of interaction of the electric quadrupole moment ( $Q$ ) of the atomic nucleus and electric field gradient (EFG) at the site of the nucleus.<sup>20-23</sup> Thus, quantum chemistry calculation of the expectation values of the components of the EFG tensor allows calculation of the components of the NQCC tensor. The NQCC of a nucleus is a perfect criterion for determination of charge density on a nucleus. In the present paper, calculated NQCCs of <sup>2</sup>H nuclei in a unit cell of nanocrystal of Mg(AlH<sub>4</sub>)<sub>2</sub> and some pressure-induced structural transitions of this compound were used to explore the electronic structure and steric factors controlling Al–H bond strength of these compounds.

## 2. COMPUTATIONAL DETAILS

Experimentally established nanocrystal structure data for  $\alpha$ -Mg(AlH<sub>4</sub>)<sub>2</sub> were used as input (Figure 1). Experimental structural data for  $\beta$ - and  $\gamma$ -Mg(AlH<sub>4</sub>)<sub>2</sub> are not available, but the calculated findings from reference are included in Table 1.<sup>13,19</sup> A unit cell of  $\beta$ -Mg(AlH<sub>4</sub>)<sub>2</sub> and  $\gamma$ -Mg(AlH<sub>4</sub>)<sub>2</sub> nanocrystals are shown in Figures 2 and 3.

Table 1: Structural parameters for Mg(AlH<sub>4</sub>)<sub>2</sub> nanocrystals in ambient and high-pressure phases.

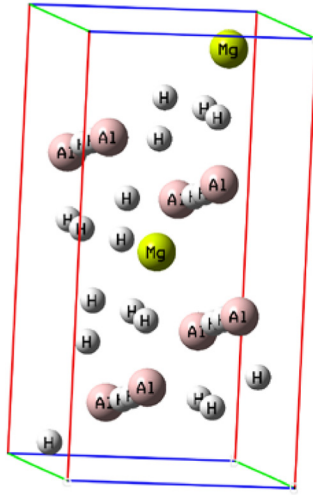
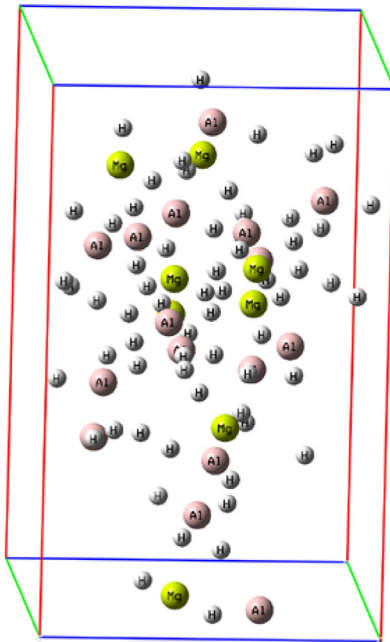
| Structure  | Lattice constants, Å <sup>o</sup> | Internal parameters           |
|--|-----------------------------------|-------------------------------|
| $\alpha$ -Mg(AlH <sub>4</sub> ) <sub>2</sub><br>( <i>p-3m1</i> ) | a = 5.208                         | Mg: 0.0000, 0.0000, 0.0000    |
|  | b = 5.839                         | Al: 0.3333, 0.6667, 0.6991    |
|  |                                   | H1: 0.3333, 0.6667, 0.4242    |
|  |                                   | H2: 0.1671, -0.1671, 0.8105   |
| $\beta$ -Mg(AlH <sub>4</sub> ) <sub>2</sub><br>( <i>C2/m</i> )   | a = 9.027                         | Mg: 0.0000, 0.0000, 0.0000    |
|  | b = 5.194                         | Al: 0.3273, 0.0000, 0.2908    |
|  | c = 6.073                         | H1: 0.0941, -0.2548, 0.8207   |
|  | $\beta$ = 89.55                   | H2: 0.1601, 0.0000, 0.2036    |
|  | H3: 0.3341, 0.0000, 0.5496        |                               |
| $\gamma$ -Mg(AlH <sub>4</sub> ) <sub>2</sub><br>( <i>pbca</i> )  | a = 12.722                        | Mg: 0.1126, -0.4807, 0.2032   |
|  | b = 8.827                         | Al1: -0.0557, -0.2275, 0.0248 |
|  | c = 8.588                         | Al2: 0.1509, -0.1251, 0.3015  |
|  |                                   | H1: -0.0148, -0.3593, 0.1417  |
|  |                                   | H2: 0.1383, 0.3860, 0.3892    |
|  |                                   | H3: 0.1292, 0.3217, 0.0972    |
|  |                                   | H4: 0.0375, -0.3558, 0.4325   |
|  |                                   | H5: 0.1584, -0.0938, 0.4856   |
|  | H6: 0.0298, -0.1028, 0.2416       |                               |
|  | H7: 0.1878, -0.2944, 0.2599       |                               |
|  | H8: 0.2238, -0.0082, 0.2057       |                               |

The HF/3-21G computational model as implemented in the Gaussian software package has been shown to be effective for efficient and accurate calculation of deuterium NQCC tensors.<sup>24-27</sup> We report here the results of calculations made for the NQCC tensors using this model as implemented in the Gaussian 03.<sup>24</sup>

## 2.1 Evaluations of NQCCs

NQR spectroscopy or zero Field NMR is a chemical analysis technique mediated by the interaction of the electric field gradient (EFG) with the quadrupole moment of the nuclear charge distribution.<sup>22</sup> Briefly, the electric field gradient at the nucleus due to its external charges is conveniently described using spatial derivatives of the corresponding electrostatic potential,  $V$ , evaluated at the nucleus:

$$eq_{ij} = \frac{\partial^2 V}{\partial i \partial j} \quad i, j = X, Y, Z \quad (1)$$

Figure 2: Crystal structure of  $\beta$ -Mg(AlH<sub>4</sub>)<sub>2</sub> modification.Figure 3: Crystal structure of  $\gamma$ -Mg(AlH<sub>4</sub>)<sub>2</sub> modification.

Thus, the EFG can be described by a real, symmetric, traceless  $3 \times 3$  tensor that in the principal axes system the components satisfy that:  $|q_{zz}| \geq |q_{yy}| \geq |q_{xx}|$ . A non-zero electric quadrupole moment arises for nuclei that are classically non

spherical. Values of  $Q$  are conveniently expressed in units of  $10^{-24} \text{ cm}^2 = 1 \text{ barn}$ . Nuclear quadrupole coupling constant can be calculated using:

$$\chi = \frac{e^2 Q q_{zz}}{h} \quad (2)$$

where  $h$  is the Planck's constant,  $Q$  is nuclear electric quadrupole moment and  $q_{zz}$  is the Z component of the EFG tensor in the principal axes system.<sup>23</sup>

Similar to the many previous studies, here we assumed that the nuclear electric quadrupole moments act as a simple constant or scaling parameter, and we do not parameterise it.<sup>25-27</sup> Among the wide range of published standard values of  $Q(^2H)$ , we selected  $Q(^2H) = 2.86 \text{ mb}$  reported by Pyykko.<sup>28</sup> It is evident that since the bond properties depend on electrons, it is possible to replace hydrogen atoms by deuterium, assuming no structural changes will occur.

### 3. RESULTS AND DISCUSSION

Calculated NQCCs of nuclei seem to be an appropriate tool for better understanding of the electronic structure of compounds. NQCC is a proper criterion for the charge density of atoms. It is essential to calculate the electric field gradient (EFG) tensor at a nucleus to achieve theoretical calculation of NQCCs. According to NQCC expression, NQCC of nuclei is directly proportional to  $q_{zz}$ .

Charge density on the nucleus and symmetry of EFG around the quadrupolar nucleus are effective factors in the values of  $q_{zz}$ . It is evident that the importance of NQCCs is to be found in the different values of the field gradient for the same nucleus in different molecules. Nucleus with higher charge density has greater  $q_{zz}$  and consequently larger  $\chi$ . In this present work, the calculated NQCCs of hydrogens of pressure-induced phases of magnesium alanate were studied to find a possible relationship between their electronic structures and their hydrogen desorption ability. NQR parameters are highly sensitive to local charge distribution. These calculations worked and since there is no experimental data on NQCCs of considered compounds, the results of these calculations were applied in qualitative predictions.

#### 3.1 Study of the Charge Density of Hydrogen Atoms in $\alpha$ -, $\beta$ - and $\gamma$ -Mg(AlH<sub>4</sub>)<sub>2</sub>

The  $\alpha \rightarrow \beta \rightarrow \gamma$  transition under high pressure is believed to be feasible for Mg(AlH<sub>4</sub>)<sub>2</sub>. The mechanism of the high-pressure structural transition was described by analysing the variation in their structural and electronic structures by Hu et al.,

and it was found that all the  $\alpha$ ,  $\beta$  and  $\gamma$  phases exhibit a common nonmetallic feature and it's a great source for hydride ions.<sup>19</sup>

The results from the calculated density of states (DOS) for  $\alpha$ -,  $\beta$ - and  $\gamma$ -Mg(AlH<sub>4</sub>)<sub>2</sub> is consistent with the ionic bonding between Mg and the AlH<sub>4</sub> subunit.<sup>19</sup> Mg(AlH<sub>4</sub>)<sub>2</sub> is an ionic compound comprised of Mg<sup>2+</sup> and AlH<sub>4</sub><sup>-</sup>. It is a great source for hydride ions. Aluminium has a low electronegativity. Therefore, the Al-H bond is very polarised with Al being positive and H being negative. In order to form a binding, the electrical charge must be transferred from aluminium atom to hydrogen. For a strong binding the mentioned charge transfer must be significant and more complete.

As it has been shown in previous studies, the NQCCs parameters at a considered coordinated atom are sensitive indicators of binding to another centre, so that rather detailed inferences regarding the extent of electron transfer can be obtained from the NQR data of this nucleus.<sup>25-27</sup> In this work, Al-H bond strength in various modifications of Mg(AlH<sub>4</sub>)<sub>2</sub> unit cell was studied using calculated NQCCs. The results are shown in Table 2.

From expression  $\chi = e^2 Q q_{zz} / h$ , it is obvious that NQCC of nuclei is directly proportional to  $q_{zz}$ . Thus larger <sup>2</sup>H-NQCC is equal to stronger Al-H bond.

Table 2 shows that in  $\gamma$ -Mg(AlH<sub>4</sub>)<sub>2</sub>, some calculated <sup>2</sup>H-NQCCs are smaller than 10 KHz while in  $\alpha$ - and  $\beta$ - Mg(AlH<sub>4</sub>)<sub>2</sub> some <sup>2</sup>H-NQCCs about 500 KHz and 1000 KHz are seen. Small <sup>2</sup>H-NQCCs in  $\gamma$ -Mg(AlH<sub>4</sub>)<sub>2</sub> are related to hydrogen atoms with low charge density. In other words, Al-H bonds in  $\gamma$ -Mg(AlH<sub>4</sub>)<sub>2</sub> nanocrystal is weaker than others and the charge transfer from Al to hydrogen atom is less than the others. Therefore, these hydrogens have weaker bonds with Al. It is expected that in the  $\gamma$ -Mg(AlH<sub>4</sub>)<sub>2</sub> phase, hydrogen atoms can be removed easier and the  $\gamma$  phase stands out as a promising candidate for hydrogen storage and this high-pressure induced phase has easier condition for dehydrogenation.

### 3.2 Comparison of Dehydrogenation Ability of Pressure-Induced Phases of Mg(AlH<sub>4</sub>)<sub>2</sub> using Calculated Enthalpies

Dehydrogenation reaction enthalpies are based on the dehydrogenation down to the dihydride:



Table 2: Calculated  $^2\text{H}$ -NQCCs in considered unit cells.

| Hydrogen                           | $\chi_{\text{H}}/\text{KHz}$ | Hydrogen                          | $\chi_{\text{H}}/\text{KHz}$ | Hydrogen                           | $\chi_{\text{H}}/\text{KHz}$ | Hydrogen | $\chi_{\text{H}}/\text{KHz}$ |
|------------------------------------|------------------------------|-----------------------------------|------------------------------|------------------------------------|------------------------------|----------|------------------------------|
| $\alpha\text{-Mg}(\text{AlH}_4)_2$ |                              | $\beta\text{-Mg}(\text{AlH}_4)_2$ |                              | $\gamma\text{-Mg}(\text{AlH}_4)_2$ |                              |          |                              |
| H4                                 | 476.06                       | H11                               | 15.24                        | H25                                | 109.27                       | H59      | 120.52                       |
| H5                                 | 476.06                       | H12                               | 120.14                       | H26                                | 112.72                       | H60      | 92.48                        |
| H6                                 | 11.94                        | H13                               | 78.24                        | H27                                | 105.92                       | H61      | 128.85                       |
| H7                                 | 108.62                       | H14                               | 86.09                        | H28                                | 84.28                        | H62      | 93.50                        |
| H8                                 | 11.96                        | H15                               | 69.38                        | H29                                | 78.08                        | H63      | 121.97                       |
| H9                                 | 11.94                        | H16                               | 35.72                        | H30                                | 112.18                       | H64      | 91.43                        |
| H10                                | 108.62                       | H17                               | 42.54                        | H31                                | 110.21                       | H65      | 90.66                        |
| H11                                | 11.96                        | H18                               | 70.35                        | H32                                | 85.66                        | H66      | 84.05                        |
|                                    |                              | H19                               | 116.27                       | H33                                | 82.16                        | H67      | 100.80                       |
|                                    |                              | H20                               | 92.15                        | H34                                | 97.70                        | H68      | 83.48                        |
|                                    |                              | H21                               | 87.29                        | H35                                | 84.35                        | H69      | 84.09                        |
|                                    |                              | H22                               | 76.97                        | H36                                | 3.40                         | H70      | 84.50                        |
|                                    |                              | H23                               | 127.25                       | H37                                | 99.97                        | H71      | 101.03                       |
|                                    |                              | H24                               | 77.95                        | H38                                | 95.97                        | H72      | 83.91                        |
|                                    |                              | H25                               | 83.29                        | H39                                | 88.61                        | H73      | 118.45                       |
|                                    |                              | H26                               | 138.47                       | H40                                | 74.65                        | H74      | 111.90                       |
|                                    |                              | H27                               | 1285.98                      | H41                                | 1.88                         | H75      | 117.86                       |
|                                    |                              | H28                               | 1295.17                      | H42                                | 102.59                       | H76      | 118.00                       |
|                                    |                              | H29                               | 1288.11                      | H43                                | 8.36                         | H77      | 114.01                       |
|                                    |                              | H30                               | 1291.16                      | H44                                | 81.05                        | H78      | 110.61                       |
|                                    |                              | H31                               | 1288.11                      | H45                                | 30.35                        | H79      | 115.58                       |
|                                    |                              | H32                               | 1290.88                      | H46                                | 101.45                       | H80      | 117.56                       |
|                                    |                              | H33                               | 1312.78                      | H47                                | 4.11                         | H81      | 102.64                       |
|                                    |                              | H34                               | 1275.91                      | H48                                | 79.53                        | H82      | 89.23                        |
|                                    |                              |                                   |                              | H49                                | 10.79                        | H83      | 101.32                       |
|                                    |                              |                                   |                              | H50                                | 13.02                        | H84      | 102.30                       |
|                                    |                              |                                   |                              | H51                                | 106.23                       | H85      | 91.54                        |
|                                    |                              |                                   |                              | H52                                | 9.76                         | H86      | 93.23                        |
|                                    |                              |                                   |                              | H53                                | 10.73                        | H87      | 89.55                        |
|                                    |                              |                                   |                              | H54                                | 13.99                        | H88      | 98.67                        |
|                                    |                              |                                   |                              | H55                                | 106.32                       |          |                              |
|                                    |                              |                                   |                              | H56                                | 9.83                         |          |                              |
|                                    |                              |                                   |                              | H57                                | 83.75                        |          |                              |
|                                    |                              |                                   |                              | H58                                | 93.28                        |          |                              |



MgH<sub>2</sub> has four different phases.  $\alpha$ -MgH<sub>2</sub> at 2.5 GPa,  $\gamma$ -MgH<sub>2</sub> at ambient pressure (after pressure release),  $\beta$ -MgH<sub>2</sub> at 8.56 GPa, and  $\delta$ -MgH<sub>2</sub> at 15.36 GPa. This point was considered for enthalpy calculations.  $\Delta H$  values relate to bond energies by:

$$\Delta H = \frac{\text{Energy used in bond breaking reactions}}{\text{Energy released in bond making products}} \quad (4)$$

In Table 3, calculated enthalpies of dehydrogenation reaction for one formula unit (f.u.) of  $\alpha$ -Mg(AlH<sub>4</sub>)<sub>2</sub> and other pressure-induced phases of Mg(AlH<sub>4</sub>)<sub>2</sub> were compared.

Table 3: The calculated enthalpies of dehydrogenation reaction for one formula unit, f.u. of  $\alpha$ -Mg(AlH<sub>4</sub>)<sub>2</sub> and other pressure induce phases of Mg(AlH<sub>4</sub>)<sub>2</sub>.

| Reaction  | $\Delta H$ (a.u/f.u.) | Pressure range (GPa) |
|---|-----------------------|----------------------|
| $\alpha$ -Mg(AlH <sub>4</sub> ) <sub>2</sub> (s) $\rightarrow$ MgH <sub>2</sub> (s)+2Al(s)+3H <sub>2</sub> (g)<br>( <i>p-3ml</i> ) <i>P42 / mnm</i> | 1643.5                | < 0.67               |
| $\beta$ -Mg(AlH <sub>4</sub> ) <sub>2</sub> (s) $\rightarrow$ MgH <sub>2</sub> (s)+2Al(s)+3H <sub>2</sub> (g)<br>( <i>C2/m</i> ) <i>P42 / mnm</i>   | -4.58                 | 0.67                 |
| $\gamma$ -Mg(AlH <sub>4</sub> ) <sub>2</sub> (s) $\rightarrow$ MgH <sub>2</sub> (s)+2Al(s)+3H <sub>2</sub> (g)<br>( <i>pbca</i> ) <i>Pa3</i>        | -2746.12              | 10.28                |

Inspection of Table 3 shows that  $\Delta H$  value of  $\gamma$ -Mg(AlH<sub>4</sub>)<sub>2</sub> is more negative than other considered phases and in this case the energy used for the bond breaking of  $\gamma$ -Mg(AlH<sub>4</sub>)<sub>2</sub> is smaller than the energy released in the reaction, which corroborate the predicted results using calculated NQCCs.

#### 4. CONCLUSION

According to the data obtained from charge distributions, the quadrupolar parameters of nuclei can be used as a useful tool to understand the electronic structure of the compounds. In  $\gamma$ -Mg(AlH<sub>4</sub>)<sub>2</sub>, hydrogens have small NQCC and therefore these hydrogens have weaker bonds with Al and easier dehydrogenation is expected in  $\gamma$ -Mg(AlH<sub>4</sub>)<sub>2</sub>. Comparison of calculated dehydrogenation enthalpies of Mg(AlH<sub>4</sub>)<sub>2</sub> phases verifies this point.

#### 5. ACKNOWLEDGEMENTS

This research was financially supported by Payame Noor University, Tehran, Iran.

## 6. REFERENCES

1. Zaluska, A., Zaluski, L. & Strom-Olsen, J. O. (2000). Lithium-beryllium hydrides: The lightest reversible metal hydrides. *J. Alloys Compd.*, 307, 157–166, [https://doi.org/10.1016/S0925-8388\(00\)00883-5](https://doi.org/10.1016/S0925-8388(00)00883-5).
2. Morioka, H. et al. (2003). Reversible hydrogen decomposition of  $\text{KAlH}_4$ . *J. Alloys Compd.*, 353, 310–314, [https://doi.org/10.1016/S0925-8388\(02\)01307-5](https://doi.org/10.1016/S0925-8388(02)01307-5).
3. Kang, S., Karthikeyan, S. & Lee, J. Y. (2013). Enhancement of the hydrogen storage capacity of  $\text{Mg}(\text{AlH}_4)_2$  by excess electrons: A DFT study. *Phys. Chem. Chem. Phys.*, 15, 1216–1221, <https://doi.org/10.1039/C2CP43297H>.
4. Prabhukhot Prachi, R., Wagh Mahesh, M. & Gangal Aneesh, C. (2016). A review on solid state hydrogen storage material. *Adv. Energy Power*, 4(2), 11–22.
5. Jorgensen, S. W. et al. (2016). Anisotropic storage medium development in a full-scale, sodium alanate-based, hydrogen storage system. *Int. J. Hydr. Energy*, 41(31), 13557–13574, <https://doi.org/10.1016/j.ijhydene.2016.05.057>.
6. Kircher, O. & Fichtner, M. (2005). Kinetic studies of the decomposition of  $\text{NaAlH}_4$  doped with a Ti-based catalyst. *J. Alloys Compd.*, 404–406, 339–342, <https://doi.org/10.1016/j.jallcom.2004.11.121>.
7. Leon, A. et al. (2009). Fluorescence XAFS study of  $\text{NaAlH}_4$  doped with a Ce-based precursor. *Phys. Chem. Chem. Phys.*, 11(39), 8829–8834, <https://doi.org/10.1039/b903272j>.
8. Fichtner, M. et al. (2003). Small Ti clusters for catalysis of hydrogen exchange in  $\text{NaAlH}_4$ . *Nanotechnol.*, 14(7), 778–785, <https://doi.org/10.1088/0957-4484/14/7/314>.
9. Pozzo, M. & Alfe, D. (2009). Hydrogen dissociation and diffusion on transition metal ( $\frac{1}{4}\text{Ti}$ , Zr, V, Fe, Ru, Co, Rh, Ni, Pd, Cu, Ag)-doped  $\text{Mg}(0001)$  surfaces. *Int. J. Hydr. Energy*, 34(4), 1922–1930, <https://doi.org/10.1016/j.ijhydene.2008.11.109>.
10. Opalka, S. M. & Anton, D. L. (2003). First principles study of sodiumealuminum-hydrogen phases. *J. Alloys Compd.*, 356–357, 486–489, [https://doi.org/10.1016/S0925-8388\(03\)00364-5](https://doi.org/10.1016/S0925-8388(03)00364-5).
11. Arroyo, D. M. E. & Ceder, G. (2004). First principles investigations of complex hydrides  $\text{AMH}_4$  and  $\text{A}_3\text{MH}_6$  (A  $\frac{1}{4}$  Li, Na, K,  $\text{M}^{\frac{1}{4}}$  B, Al, Ga) as hydrogen storage systems. *J. Alloys Compd.*, 364(1–2), 6–12, [https://doi.org/10.1016/S0925-8388\(03\)00522-X](https://doi.org/10.1016/S0925-8388(03)00522-X).
12. Fichtner, M. & Fuhr, O. (2003). Magnesium alanate—a material for reversible hydrogen storage. *J. Alloys Compd.*, 356–357, 418–422, [https://doi.org/10.1016/S0925-8388\(02\)01236-7](https://doi.org/10.1016/S0925-8388(02)01236-7).

13. Fichtner, M. et al. (2003). The structure of magnesium alanate. *Inorg. Chem.*, 42, 7060–7066, <https://doi.org/10.1021/ic034160y>.
14. Fossdal, A. et al. (2005). Determination of the crystal structure of  $\text{Mg}(\text{AlH}_4)_2$  by combined X-ray and neutron diffraction. *J. Alloys Comp.*, 387, 47–51, <https://doi.org/10.1016/j.jallcom.2004.06.050>.
15. van Setten, M. J. et al. (2005). Ab initio study of  $\text{Mg}(\text{AlH}_4)_2$ . *Phys. Rev. B*, 72, 73107, <https://doi.org/10.1103/PhysRevB.72.073107>.
16. Spano, E. & Bernasconi, M. (2005). Ab initio study of the vibrational properties of  $\text{Mg}(\text{AlH}_4)_2$ . *Phys. Rev. B*, 71, 174301, <https://doi.org/10.1103/PhysRevB.71.174301>.
17. Hou, Z. F. (2006). First-principles investigation of  $\text{Mg}(\text{AlH}_4)_2$  complex hydride. *J. Power Sour.*, 159, 111–115, <https://doi.org/10.1016/j.jpowsour.2006.04.015>.
18. Claudy, P., Bonnetot, B. & Letoffe, J. M. (1979). Preparation et proprietes physico-chimiques de l'hydrure d'aluminium  $\text{AlH}_3\gamma$ . *J. Thermal. Anal.*, 15, 129–139, <https://doi.org/10.1007/BF01910204>.
19. Hu, C. H. et al. (2007). First-principles investigations of the pressure-induced structural transitions in  $\text{Mg}(\text{AlH}_4)_2$ . *J. Phys. Condens. Matter.*, 19, 176205, <https://doi.org/10.1088/0953-8984/19/17/176205>.
20. Leach, A. R. (1997). *Molecular modeling principles and applications*. Singapore: Longman.
21. Lucken, E. A. C. (1969). *Nuclear quadrupole coupling constant*. London: Academic Press.
22. Graybeal, J. D. (1988). *Molecular spectroscopy*. Singapore: McGraw-Hill.
23. Slichter, C. P. (1992). *Principles of magnetic resonance*. New York: Springer.
24. Frisch, M. J. et al. (2003). *GAUSSIAN 03*. Pittsburgh, PA: Gaussian Inc.
25. Rafiee, M. A. & Partoee, T. (2011). Investigation of the binding affinity between styrylquinoline inhibitors and HIV integrase using calculated nuclear quadrupole coupling constant (NQCC) parameters (a theoretical ab initio study). *Bull. Korean Chem. Soc.*, 32, 208–212, <https://doi.org/10.5012/bkcs.2011.32.1.208>.
26. Rafiee, M. A. (2015). Comparison of metal additives and boron atom on  $\text{MgH}_2$  absorbing-desorbing characteristics using calculated NQCCs. *Int. J. Nano Dimens.*, 6(3), 289–295.
27. Rafiee, M. A. (2014). A theoretical study of  $\text{MgH}_2$  ambient and high-pressure phases using NQCC parameters. *Russ. J. Phy. Chem. A.*, 88(13), 2359–2362, <https://doi.org/10.1134/S0036024414130172>.
28. Pyykko, P. (2001). Spectroscopic nuclear quadrupole moments. *Mol. Phys.*, 99, 1617–1629, <https://doi.org/10.1080/00268970110069010>.